WALL STATE EFFECTS ON Cl_2 POLY-SI RIE: REAL-TIME MEASUREMENTS, MECHANISMS, AND FEEDBACK CONTROL SOLUTIONS

Pete I. Klimecky, Jessy W. Grizzle, and Fred L. Terry, Jr.
University of Michigan/EECS Dept. , Rm 2408
1301 Beal Ave, Ann Arbor, MI 48109
crown@eecs.umich.edu

Abstract

The wall-state of reactive ion etch tools is known to strongly affect etch results, and previous studies show neutral species concentrations vary with chamber seasoning. This paper presents the first simultaneous, real-time, *in situ* measurements of etch rates, plasma electron density (n_e), and Cl neutral actinometry data during high-density Cl_2 reactive ion etching of poly-Si. Moreover, we demonstrate a real-time feedback control system that corrects for plasma density variations and eliminates the "first wafer" effect observed after chamber fluorination/cleaning. Following chamber fluorination, transient density changes, measured with a microwave resonance cavity technique called BroadBand RF, show a significant (~38%) increase in electron plasma density during a 60s Cl_2 etch. Variations in real-time poly-Si etch rate correlate closely with the BroadBand signals. Observed real-time variations are compensated using a proportional-integral (PI) feedback control algorithm, where BroadBand peak frequency is the system output variable and TCP power is the system actuator. PI control restores both nominal density and poly-Si real-time etch rate. These results are fully consistent with a significant body of experimental and theoretical work suggesting that high density plasma Cl_2 etching of Si is ion-dominated, however they are the first to clearly demonstrate these connections to real-time etch rate variations and provide the first demonstration of feedback control correction for wall-state drift.

Introduction

High yield, high throughput processing is of primary importance in modern semiconductor manufacturing. With current CD design rules shrinking below 0.13μm, the demand for consistent reactive ion etching (RIE) steps is crucial to increasing overall yield. To this end, modern RIE process manufacturing requires multiple test wafers, frequent plasma clean steps, and frequently scheduled chamber maintenance in order to reduce variance and maintain a consistent manufacturing environment. Tighter controls on the root causes of etch variance would help improve fabrication tolerance limits.

One area of ongoing interest regarding the source of process variations over time concerns the chamber wall condition [1-6]. Experimental measurements of Cl neutral (n_{Cl}) transients and correlations of these transients with chamber conditions have been reported [1,2]. Variations of Cl^+ ion concentrations (n_{Cl+}) with n_{Cl} recombination loss rates has been suggested in simulations[3]. Different rate limiting reactions at the wall surface have been proposed as reasons for changes in n_{Cl} concentrations, dependent upon whether an SiO_2 or SiO_xCl_y layer has built up over time, or whether the walls have been stripped of oxide layers by a previous fluorine-containing plasma clean step.

We will show that *both* n_{Cl} *and* n_{Cl+} densities vary significantly during an etch run, and that these variations are closely related to the chamber seasoning. We demonstrate that for this chemistry the etch rate variation is dominated by ion density variation rather than the neutral Cl variation. Further, we will show that using closed-loop feedback control to correct for plasma density transients flattens the etch rate even though there is still variation in the n_{Cl} concentration.

In addition, we will show a significant extension of the Cl_2 actinometry work of Donnelly [2]. Using our *in situ* plasma density estimates, we will show that the time variations of the Cl and Ar optical emission line intensities can be accurately modeled by the time-variation of n_e and the dissociation fraction of Cl_2. We will demonstrate a test for constant electron temperature (T_e) using a combination of our n_e measurement and the n_{Cl} OES signal. We will show that during feedback control of n_e, T_e is still time-varying, thus complicating the interpretation of Cl actinometry results.

Experimental Setup

All experiments etch undoped poly-Si wafers in a Lam Research 9400SE reactor. 150mm wafers are electrostatically chucked at 650V, with 100W bias forward power in all experiments.

Three external sensors monitor the process: 1) BroadBand RF [7] peak absorption frequencies indicate changes in the plasma density; 2) Real-Time Spectroscopic Ellipsometry (RTSE) measures *in situ* film thickness and etch rate data; 3) Optical Emission Spectroscopy (OES) records glow discharge intensity of characteristic emission lines of Cl and Ar at 822.2 and 750.4nm, respectively. All input and control signals operate at a sampling frequency of 4Hz.

The BroadBand RF peak resonance absorption sensor [8] is a small microwave antenna housed in a protective quartz sheath, inserted about 3" into the chamber sidewall. The sensor measures the complex reflection coefficient vs. frequency from 100 MHz to 3 GHz. Measured peak absorption power has specific resonance frequencies dependent upon the chamber geometry and the plasma-loaded permitivity of the cavity. These resonances are directly related to the electron plasma frequency, ω_{pe}, and are thus directly related to the square root of n_e [9].

Experimental Goals

Two sets of experiments are performed. In the first, three 60s runs compare three different etch conditions: 1) starting from a chlorine-seasoned chamber wall (termed Cl-prep), a nominal chlorine etch establishes steady state conditions; 2) an identical chlorine recipe initiates after a fluorine-cleaned chamber wall (termed F-prep) to observe open-loop etch transient behavior; and 3) starting again from an F-prep chamber wall, a chlorine etch utilizing closed-loop density control compensates for transient effects.

In the second experiment, the chamber is cleaned once in a fluorine environment, to establish the F-prep wall state, followed by three successive 30s Cl_2 etches. These three etches are first performed using open-loop recovery, with no transient compensation. Next, the chamber is again fluorine-cleaned and three new 30s Cl_2 etches are performed using closed-loop feedback compensation to maintain a constant density.

Experimental Results

Figure 1a shows a real-time comparison between the three etch conditions for the first set of experiments: nominal etch rate in a stable Cl-prep chamber, open-loop etch rate starting from an F-prep chamber, and closed-loop etch rate starting from an F-prep chamber. Figure 1b shows a similar comparison for the corresponding density indicator (the second BroadBand peak frequency ω_{h2}). Note the significant drop in both etch rate and density at the start of the open loop runs. Clearly the F-prep step to remove halogenated oxides from the chamber surfaces has a large effect on plasma density as well as plasma chemistry. In the 60s time allotted for the open loop etch, the BroadBand frequency and etch rate did not have sufficient time to fully recover to their respective nominal values. Full recovery time back to nominal Cl-prep conditions is ~5mins with the nominal recipe.

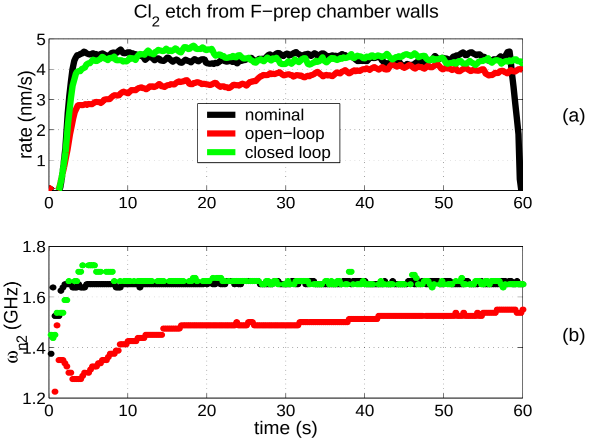

Figure 1. Nominal, open-loop, & closed-loop response for a) etch rate and b) BroadBand peak.

For the second set of experiments with three successive 30s etches, total etched material for the first open-loop set is plotted sequentially in Fig. 2a. As expected from the real-time results of Figure 1, the total etched material over a 30s process is found to increase for each wafer, which clearly demonstrates the common first wafer effect. The etch rate is increasing for each run as the wall seasons with oxy-chloride compound and the recombination rate goes down. Over three wafers during standard open-loop conditions, the total etch depth increases by ~150Å due to the dynamic wall interactions in the chamber.

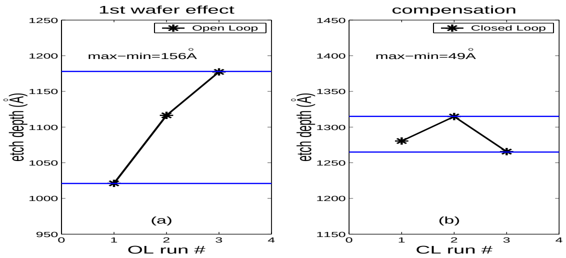

Figure 2. Total etched material after 30s Cl_2 etch following F-prep clean a) open-loop b)closed-loop.

The results of the closed-loop set are shown in Fig. 2b for comparison. The (max-min) difference is greatly reduced, by a factor of three, to ~50Å, vs. the corresponding etches performed in open loop.

To compare density changes with OES, let ω_{BB} equal the BroadBand peak frequency. Since $n_e \propto \omega_{BB}^2$ [9], the optical emission spectroscopy signals from the Cl and Ar emission lines can be modeled as:

$$I_{Ar} = K_1(T_e, \lambda_{Ar})\omega_{BB}^2 P\left[f_0 / \left(1 + d(1 - f_0)\right)\right] \quad (1)$$

$$I_{Cl} = K_2(T_e, \lambda_{Cl})\omega_{BB}^2 P\left[\left(2d(1 - f_0)\right) / \left(1 + d(1 - f_0)\right)\right] \quad (2)$$

where the K_1 and K_2 functions contain the activation integrals over the electron energy distribution function and excitation cross-sections, optical system factors, the scale factor between ω_{BB} and n_e, as well as ideal gas scaling between pressure (P) and the molar gas fractions. The term d is the fraction of molecular Cl_2 dissociated into atomic Cl, and f_0 is the mole fraction of Ar in the feed gas. Eqs. (1) and (2) are coupled through the dissociation fraction d and are related to the actinometric ratio by:

$$\left(I_{Cl} / I_{Ar}\right) = 2d(K_2 / K_1(1 - f_D)) / f_D \quad (3)$$

Previous quantitive work on Cl actinometry used the assumption that a constant I_{Ar} signal is due to constant plasma conditions. In the presence of varying Cl_2 dissociation, this cannot be true due to varying dilution of Ar by Cl atoms. However, with n_e and the Ar fraction varying in opposite directions, a relatively constant I_{Ar} may result. Assuming a constant T_e for $t \geq 5$s during an open-loop, F-cleaned run, we fit K_1 and K_2 and obtain the self-consistent fits to I_{Ar} and I_{Cl} shown in Figure 3, and obtain the quantitative dissociation fraction, d, also shown in this plot.

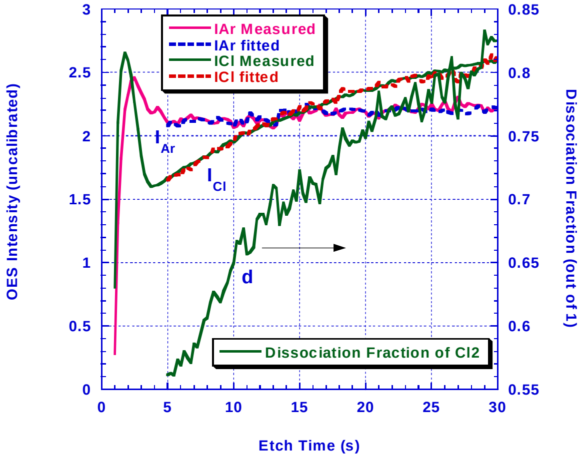

Figure 3. Measured and fitted I_{Ar} and I_{Cl} signals and Cl_2 dissociation fraction d, assuming constant T_e and equations 1-3.

In the presentation, we will show that the relationship of the Cl^+ ion density to the Cl neutral density yield the useful result that $\left(\omega_{BB}^4 / I_{Cl}\right)$ varies with T_e. For the fits shown in Figure 3 (with K_1=3.7764 ±0.1792 and K_2=0.13677 ± 0.009411), this ratio is nearly constant for $t \geq 5$s. For the closed-loop feedback controlled runs, this ratio shows the electron temperature is increased by the additional compensating TCP power and decreases as the TCP power is reduced by the control system. This makes the actinometry data from this run more problematic to interpret quantitatively (since we have an indicator of T_e but not a direct measure). However, at this time, our analysis of the closed-loop data shows that the atomic Cl concentration is increased by the added TCP power, but the losses due to wall recombination are not fully corrected by the stabilization of n_e.

We suggest the following model for our results:

1. The Cl neutral concentration is reduced due to recombination on F-cleaned chamber surfaces.
2. n_{Cl+} is reduced due to lower availability of n_{Cl} precursors. Quasi-neutrality thus reduces n_e and Si etch rates decrease due to lower ion bombardment.
3. In successive runs without F-cleans, the reactor walls season and both Cl neutral and Cl^+ ion concentrations approach constant values.
4. Closed-loop feedback control of n_e through the TCP power compensates for n_{Cl+} losses by increasing T_e. The Cl ionization rate increases more dramatically than the Cl_2 dissociation rate due to the higher threshold energy for ionization.
5. Etch rate is more constant using this control action even though n_{Cl} is not fully corrected. There are presumably enough n_{Cl} species under all the explored conditions to keep the surface fully Cl-saturated, and thus making the etch rate ion limited.

Acknowledgements

This work was supported in part by AFOSR/ARPA MURI Center under grant #F49620-95-1-0524 and NIST ATP #70NANB8H4067.

References

[1] E. Aydil et al, *JVSTA*, **20**, No. 1 (Jan/Feb 2002)
[2] V. M. Donnelly, *JVSTA*, **14**, No. 4 (1996)
[3] G. I. Font et al, *JVSTA*, **16**, No. 4 (Jul/Aug 1998)
[4] G. Zau & H. Sawin, *J. El. Chem. Soc.* **139**, (1992)
[5] A Watts & W Varhue, *App. Phys. Let.*, **61**, (1992)
[6] M. Malyshev and V. M. Donnelly, *J. Appl. Phys.*, **88**, pp 6207 (2000)
[7] C. Garvin, D. Grimard, J. Grizzle, *Char & Metrology for ULSI Tech.*, **449**, pp 442-6 (1998)
[8] C. Garvin & J. Grizzle, *JVSTA*, **18**, 4 (2000)
[9] P. Klimecky, J. Grizzle, F. Terry Jr., *Proc. AEC/APC XIV Symposium*, (2002)